Nano Energy 84 (2021) 105908

Contents lists available at ScienceDirect

Nano Energy

journal homepage: http://www.elsevier.com/locate/nanoen

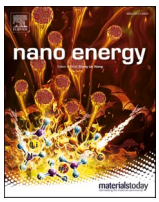

Unveiling micro internal short circuit mechanism in a 60 Ah high-energy-density Li-ion pouch cell

Xiaopeng Qi [a,c], Bingxue Liu [a,c], Jing Pang [a,c,d], Fengling Yun [a,c], Rennian Wang [a,c], Yi Cui [a,c], Changhong Wang [b], Kieran Doyle-Davis [b], Chaojian Xing [a,c], Sheng Fang [a,c], Wei Quan [a,c], Bin Li [a,c], Qiang Zhang [a,c], Shuaijin Wu [a,c], Shiyang Liu [a,c], Jiantao Wang [a,c,d,*], Xueliang Sun [b,**]

[a] China Automotive Battery Research Institute Co., Ltd., No. 11 Xingke Dong Street, Huairou District, Beijing 101407, China
[b] Department of Mechanical and Materials Engineering, University of Western Ontario, 1151 Richmond St, London, Ontario N6A 3K7, Canada
[c] GRINM Group Corporation Limited (GRINM Group), No. 2 Xinjiekou Wai Street, Xicheng District, Beijing 100088, China
[d] General Research Institute for Nonferrous Metals, No. 2 Xinjiekou Wai Street, Xicheng District, Beijing 100088, China

ARTICLE INFO

Keywords:
Micro internal short circuits
Safety
Thermal runaway
Li-ion cells
Si-based anode
Ni-rich cathode

ABSTRACT

The identification, evaluation, and prevention of micro internal short circuits (ISCs) are crucial for the safety of large-capacity high-energy-density (HED) Li-ion cells. However, the evolution mechanism and the premonitory signals of the micro ISCs are not yet completely understood. Via a high-precision penetration test and accelerating rate calorimetry, we successfully trigger and investigate on-demand ISCs on a 60 Ah HED ($\geq$ 290 Wh kg^{-1}) Li-ion pouch cell with Si-based anode/Ni-rich cathode couple. Detailed behaviors of the cell components during micro ISCs, such as pinhole and crack formation, pore-closing, and rupture of the separators, as well as the destruction of positive electrodes and fusion of Al current collectors, are observed. Moreover, the correlation of these internal effects with external cell signals is identified. We demonstrate that voltage change signals, even at millivolt level, are noteworthy and can be used as premonitory signals for early warning of micro ISCs and leading indicators for predicting cell thermal runaway. The disclosed micro ISC propagation, alleviation, and acceleration mechanisms could guide the design of safe HED Li-ion cells.

1. Introduction

Vehicle electrification is sweeping the world. The pursuit of high-energy-density (HED) energy storage devices has significantly accelerated the innovation of Li-ion batteries (LIBs) [1,2], but may also have contributed to the increasing electrical vehicle (EV) accidents associated with battery thermal runaway (TR) events [3,4]. Nickel-rich Li$[Ni_{1-x-y}Co_xMn_y]O_2$ (NCM) cathodes preferred in HED cells generally react aggressively with the electrolytes [5–7]. Si-based high-capacity anodes often induce excessive solid electrolyte interphases (SEI) [8,9], which usually decompose exothermically at low temperatures [10]. Thin separators and current collectors with inferior mechanical and thermal stabilities can also render the cells prone to internal short circuits (ISCs) [11,12]. Catastrophic fire and explosion can occur due to the combustion of the carbonate electrolytes and the hydrocarbon side products [13–15].

During many Li-ion cell TR events, one process playing crucial roles is the ISCs, which can be triggered in various cell electric [16,17], mechanical [18–22], and thermal [23] abuse conditions that can cause the separator malfunction or electrode direct contact [24–26]. Severe ISCs generally lead to intense cell energy release and can ignite a cell in seconds, making the effectiveness of external cooling or other protective designs very limited. By contrast, micro ISCs are thornier as they can occur unpredictably in many situations without obvious or detectable cell abuse. Micro ISCs can be induced by lithium microstructures [27], unintentionally incorporated particle impurities, electrode laminate burrs, and many other almost inevitable latent cell quality defects, and can evolve into severe ISCs without being prevented. Recently, many pieces of evidence indicate that micro ISCs may be the underlying cause for many unexpected cell TR events, like those increasingly occurring on parked EVs. Targeted internal prevention designs are preferred and should be based on a thorough understanding of the micro ISC evolution

* Corresponding author at: China Automotive Battery Research Institute Co., Ltd., No. 11 Xingke Dong Street, Huairou District, Beijing 101407, China.
** Corresponding author.
E-mail addresses: wangjt@glabat.com (J. Wang), xsun9@uwo.ca (X. Sun).

https://doi.org/10.1016/j.nanoen.2021.105908
Received 19 December 2020; Received in revised form 15 February 2021; Accepted 16 February 2021
Available online 22 February 2021

mechanism. Advanced separators [28,29], thermally responsive materials [30], or other novel energy storage devices such as solid-state batteries [31–33] hold great promise. However, the wide application of these strategies is currently compromised by either the cost or inconvenience in manufacturing. Therefore, many automakers are having to devote intensive effort to designing and incorporating effective micro ISC early warning systems into their battery management system (BMS). To this end, a prerequisite is to correlate the external available signals to the internal ISC states and risks. Among the most available signals for the BMS, changes in current and temperature are often undetectable or delayed in micro ISCs, whereas the voltage signal theoretically responds promptly to ISC discharging, thus being a promising sensitive probe to track micro ISC events.

Nevertheless, the micro ISC evolution mechanisms are still uncovered, and the implications of the premonitory signals are also not well understood. The challenge may mainly originate from the lack of controlled ISC triggering techniques and insufficient direct experimental knowledge about micro ISCs. Severe ISCs generally leave a mess of burnt cell components only for post-mortem analysis. Several embedded-in devices such as low melting point metal [34], shape memory alloys [35], and wax-coated devices [36] have been developed to trigger ISCs. These methods, however, usually render substantial modifications and affect the true performances of the cells. In comparison, penetration tests with small nails and slow speeds are promising to minimize the mechanical effects and enhance the controllability of the ISC triggering [21,37,38]. Herein we investigate the micro ISCs in a 60 Ah Li-ion pouch cell with an extremely high energy density ($\geq$ 290 Wh kg^{-1}). Benefiting from a high-precision voltage-controlled penetration test with small (diameters of 1 mm) and slow (0.1 mm s^{-1}) nails, we managed to stimulate on-demand micro ISCs confined within 2–5 electrode pairs. Voltage drops, as important signals for the BMS, were used to control the nails and the severities of the ISCs. This method ensured the examination of the variation of the cell component morphologies, voltages, and temperatures during early-stage micro ISCs. With the accelerating rate calorimetry (ARC) test and equivalent circuit analysis, the micro ISC propagation, alleviation, and acceleration mechanisms, and the implications of external voltage and temperature signals were revealed.

2. Experimental section

2.1. The Li-ion cells

The Li-ion cells used a Li[$Ni_{0.83}Co_{0.12}Mn_{0.05}$]$O_2$ NCM cathode and a SiO_x/graphite blended anode with a capacity of ca. 500 mAh g^{-1}. A polyethylene (PE) membrane (12 μm thick) with single-side ceramic coating (3.32 μm thick) was used as the separator with the ceramic coating toward the positive electrodes in the cell. The electrolyte was 1 M $LiPF_6$ in EC/DEC/EMC (25:50:25 by weight) with FEC (7 wt%) and VC (0.5 wt%) additives. The 60 Ah cell delivered a 1/3 C rate capacity of 61.9 Ah and a high energy density of 292 Wh kg^{-1}. The voltage curves, an image, and the dimensions of the 60 Ah cell are shown in Fig. S1. A 26 Ah cell was prepared with fewer electrode laminates. The cells used in the ARC and penetration tests were all fully charged by the standardized CC-CV method (1 C rate charging to a 4.2 V cut-off voltage followed by constant-voltage charging to a 0.05 C cut-off current).

2.2. Accelerating rate calorimetry (ARC) test

An EV+ accelerating rate calorimeter (THT) and the classic heat-wait-seek mode were used in the ARC test. The cell voltage and the temperature signals were monitored by a data logger (HIOKI LR8431-30) coupled with K-type thermal couples. The start temperature was set to 50 °C; the heating step was 5 °C; the temperature rate sensitivity was 0.02 °C min^{-1}; the wait time after each heating step was 50 mins.

2.3. Nail penetration tests

An ESPEC ADST-N20 machine was used for the nail penetration tests. The cell voltage was monitored by a HIOKI 3237 Digital Hitester connected to the testing machine. And 5 mV and 10 mV voltage drops were set as cut-off signals to automatically stop the nail penetration. Three K-type thermal couples were mounted at the nail (3 mm from the nail tip), the front surface of the cell (8 mm from the penetration spot), and the back surface of the cell (right against the penetration spot), respectively. A steel nail with a diameter of 1 mm and a tip cone angle of 30° was used. The testing temperatures were 25 ± 2 °C. The speeds of the penetration were all 0.1 mm s^{-1}.

Additional experimental details, including the differential scanning calorimetry (DSC) test, characterization of the cell component morphologies, and the electrode coating layer resistances, were provided in the Supplementary Material.

3. Results and discussion

3.1. Premonitory micro ISCs in heat-induced cell thermal runaway

By creating an adiabatic condition, ARC tests are versatile in investigating the exothermic effects and are capable of triggering uniformly distributed ISCs. We herein report the first ARC investigation on a Li-ion cell with such a high capacity ($\geq$ 60 Ah) and energy density ($\geq$290 Wh kg^{-1}). As can be seen in Fig. 1a, detectable self-heating (defined as a minimum temperature rising rate of 0.02 °C min^{-1}) starts at 72.03 °C (T_{onset}), which is slightly lower than those of the other cells in the literature (~85 °C) [39]. The lower T_{onset} implies a higher self-heating risk of the cell, which is likely associated with the decomposition of the metastable phase in the SEI of the Si-based anode [40]. The onset is also consistent with the differential scanning calorimetry (DSC) analysis of the anode sample (Fig. S2). As the temperature rises to T_{SISC} (164.8 °C in Fig. 1a and b), the voltage drops abruptly from 3.972 V to 0.242 V during a short period of 0.2 s. T_{SISC} (164.8 °C) is lower than the temperatures of the exothermic peaks of the anode and cathode while higher than the melting temperature of the separator (Fig. 1d), indicating that the abrupt voltage drop is probably due to the severe large-area ISCs from the separator breakdown. The exothermic peaks of the anode sample are consistent with the literature results [41,42]. T_{SISC} (164.8 °C) is also much higher than the melting peak of the separator (140.5 °C in Fig. 1d). The reason could arise from the ceramic coating layer, which can serve as temporary self-supports and enhance the melt integrity of the separator [43].

Further examination of curves in Fig. 1a revealed the temporary voltage fluctuation that starts at T_{MISC} (142 °C in Fig. 1c), about 13.2 mins before the large voltage drop at T_{SISC} (164.8 °C). Similar observations were rarely reported. However, the significant voltage variation and the relatively long time interval from T_{MISC} to T_{SISC} may be valuable for the BMS to predict and warn of subsequent cell TR. The voltage did not reach zero, suggesting that the voltage decline is not due to the shutdown of the separator, which has been suggested by Mohamedi et al. [44]. to be capable of preventing the electrochemical activity of the cell. We speculate that the voltage fluctuation is indicative of the occurrence of micro ISCs. Recent research also predicts possible gentle or soft ISCs before the breakdown of the separators [45,46]. As temperature rises, polyolefin separators can experience behaviors such as soften, deformation, shrinkage, melting, rupture, and breakdown [11,12]. The micro ISCs in the ARC test may occur due to the mild melting of the separator and the uneven surfaces of and pressure between the electrode laminates. Micro pinholes and cracks thus formed in the separators can cause numerous tiny direct electrode contacting spots. The relatively long time interval of this stage may also be associated with the ceramic coating layer [43]. To fully explain the voltage variation, especially the voltage recoveries, however, we need additional investigation on the micro ISCs, which is provided by the nail tests.

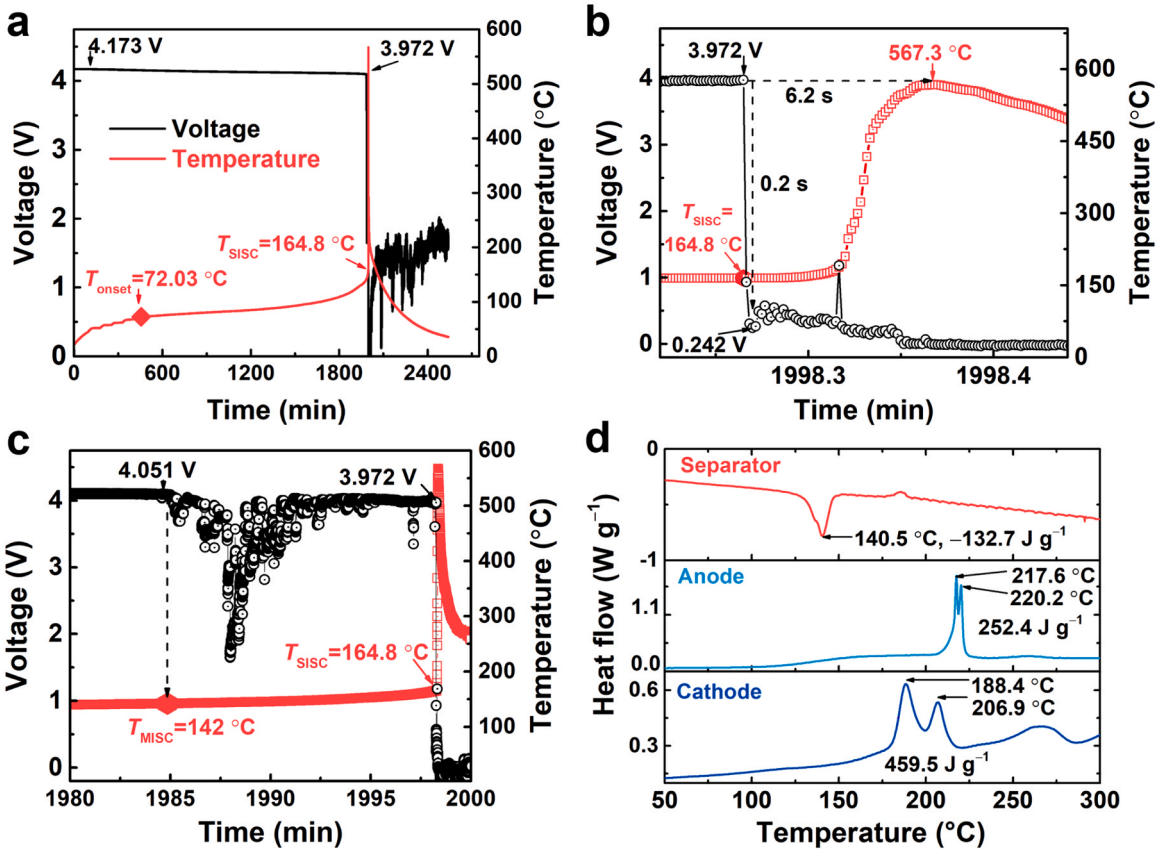

Fig. 1. (a) Voltage and temperature curves of the 60 Ah cell during the ARC test; (b), (c) enlarged sections of (a). (d) Heat flows in the differential scanning calorimetry (DSC) tests of the pristine separator, and the anode and cathode samples scratched from the laminates of fully charged cells (positive heat flows suggest exothermic effects).

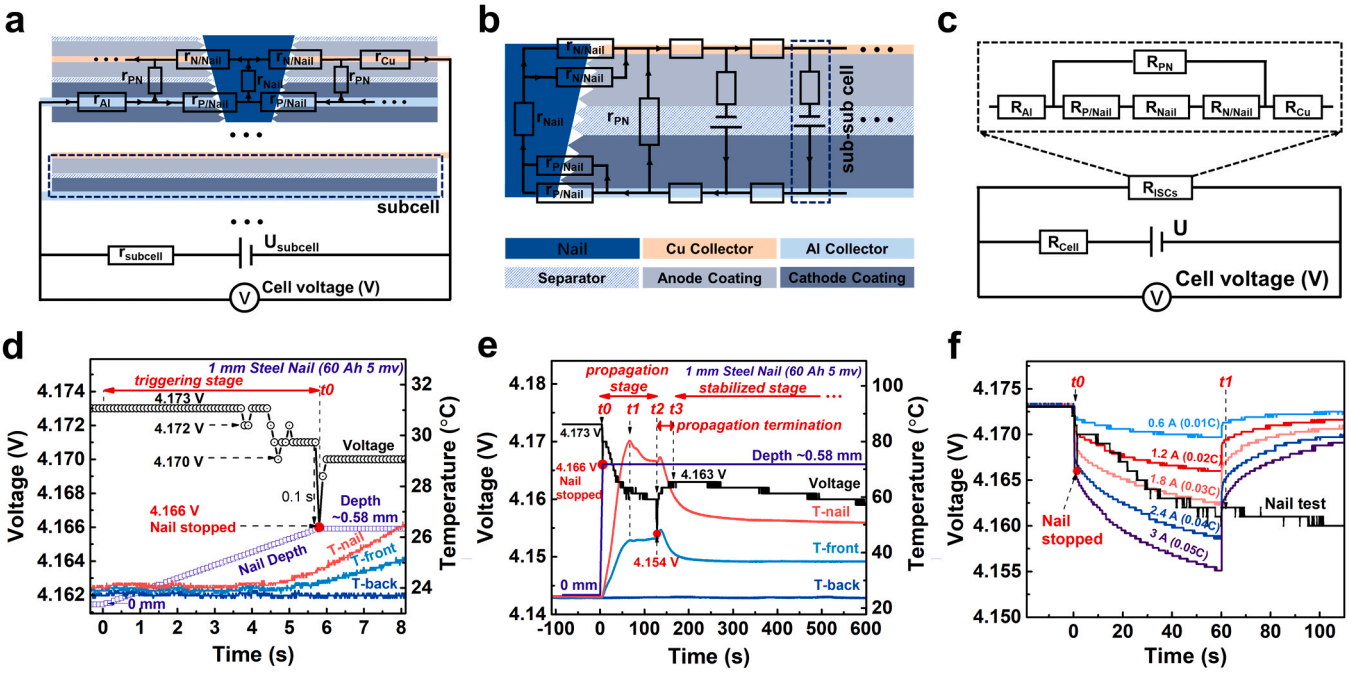

Fig. 2. Illustration of possible current paths and related resistances in (a) a shorted cell and (b) half of a shorted electrode pair. (c) The equivalent circuit diagrams. (d) and (e) The penetration depth, voltage, and temperature curves of the 60 Ah cell in the penetration test with a 5 mV cut-off voltage drop; (e) is an enlarged section of (d); T-nail, T-front, and T-back denote the temperatures at the nail, the front surface, and the back surface of the cell. (f) The voltage curves of the 60 Ah cell during the penetration test and under normal external discharging with different currents.

3.2. Micro ISC evolution to a stabilized state

3.2.1. Voltage and temperature signals

To better interpret the voltage signals and the heat generation, herein we introduce the equivalent circuit analysis. Fig. 2a–c illustrate the possible current paths, resistances, and the equivalent circuit diagram of micro ISCs triggered by nail penetration. We adopt the concept of subcell by Yokoshima et al. [21] and propose the concept of the sub-sub cell. Each subcell can be thought of as being composed of discrete sub-electrode pairs, or sub-sub cells, connected in parallel by the metal current collectors. R_{PN} reflects the ISCs from direct contact of the positive and negative electrodes, which is associated with the impairment of the separators. $R_{N/Nail}$ and $R_{P/Nail}$ represent the contact resistances at the electrode/nail interfaces, which generally contribute significantly to the total ISC resistance (R_{ISCs}) [47]. R_{Al}, R_{Cu}, and R_{Nail} represent the resistances of the Al collector, Cu collector, and the steel nail, respectively. For the present testing cell with two pairs of electrodes shorted, they are estimated to be in the magnitude of 10^{-2}–10^{-3} Ω from the dimensions and the resistivities of 1.75×10^{-8}, 2.83×10^{-8}, and 7.3×10^{-7} Ω m for Cu, Al, and Fe, respectively, and should be negligible to the total micro ISC resistance. Accordingly, the voltage drops in the metal collectors are negligible compared to that falling upon the ISC spot, and would have a negligible influence on the cell voltage measured between the current collecting tabs. Therefore, to estimate the ISC current and resistance, we can perform external discharge on an intact cell with different currents and compare the voltage curves with that under micro ISCs.

As the cell discharges due to ISCs, the measured cell voltage (V) is actually the working voltage, equaling the true open-circuit voltage (OCV, or U) less the polarization voltage drop ($\Delta V = U–V$), which is reflected by the equivalent polarization resistance, R_{Cell}. A smaller R_{ISCs} allows a larger ISC current, which would thus cause higher polarization (larger ΔV), a higher voltage decrease rate, and a higher heat generation rate. The mathematical relations between the voltages, currents, resistances, and heat generation rates are provided in the Supplementary Material.

Fig. 2d and e show the cell voltage and temperature signals during the penetration test with a 5 mV cut-off voltage drop controlling the stop of the nail. As can be seen in Fig. 2d, the nail stopped at 4.166 V, corresponding to a voltage drop of 7 mV from 4.173 V. The recorded penetration depth was 0.58 mm, indicating that the maximum diameter of the penetrated nail tip was only about 0.31 mm. The cell passed the test without fire or explosion. Two electrode pairs were penetrated, as was confirmed by examining the disassembled cell after the test. The xth layer of the separator, negative laminate, and positive laminate along the penetration direction is denoted as Sx, Nx, and Px, respectively. We define the period before the stop of the nail (at t0) as the ISC triggering stage (Fig. 2d), during which the three obvious couples of voltage drops and recoveries reflect the successive short circuits from the three electrode laminates (P1, N2, and P2). The voltage drops and recoveries may be due to the variation of the heterogeneous contact resistances. The nail movement can compress the cell components and enable compact heterogeneous contacts, leading to smaller contact resistances. Once the laminates are punctured, the release of the compression may give rise to loose contacts and larger contact resistances. The observation of these trace signals demonstrates the high precision of the test.

The period from t0 to t3 (Fig. 2e) was defined as the ISC propagation stage, during which the voltage and temperatures experience intensive variations. To estimate the magnitude of the ISC current and resistance, we externally discharging the cell at different currents and compare the voltage curves with that in the nail test (Fig. 2f). The ISC voltage curve initially overlaps with the external discharge curve at 1.2 A (0.02 C rate) while gradually gets closer to that under 1.8 A (0.03 C), which is indicative of ISC propagation possibly because of the separator melting. With the U and V, the 1.2 A current implies an estimated cell polarization equivalent resistance (R_{Cell}) of 2.5 mΩ and an ISC resistance (R_{ISCs}) of 3.5 Ω (see Eqs. (S2) and (S3)). The estimated R_{ISCs} is much larger than those from the metal current collectors and the steel nail (~10^{-2}–10^{-3} Ω), suggesting the dominant contribution from the heterogeneous contact resistances. For the positive laminates/nail interface, most of the current may be condensed at the Al current collectors, which has a much lower resistivity of 2.83×10^{-8} Ω m than that of the cathode coating layer (0.372 Ω m). Given the ultra-small Al/nail interface area (estimated to be 0.011 mm^2), the 1.2 A current implies an ultra-high Al/nail interfacial current density of 106 A mm^{-2}. The resultant localized joule heating might be sufficient to cause the fusing of the Al collector (with a low fusing point of 660 °C), which was confirmed by examining the dissembled cell. In revisiting the voltage and temperature curves, Al fusion may occur at t1 when T-nail reaches its peak. The decreased T-nail and slowed voltage decreasing rate after t1 can be attributed to the decreased ISC current and joule heating because of the disconnection of the Al/nail contact.

Interestingly, after t1, T-front did not decrease with T-nail but kept increasing at a slowed rate, which may suggest ISC spreading. At t2, an abrupt voltage drop and subsequent gradual recovery occurred with synchronized temperature peaks and subsequent declines, which implies abrupt ISC aggravation and subsequent ISC alleviation. The smooth voltage and temperature after t3 suggest that a stabilized ISC is achieved. To reveal the underlying reasons for the voltage and temperature variations, cells were disassembled after the test and the cell components were thoroughly inspected.

3.2.2. Separators and electrode laminates

We focus on the separators firstly as they play critical roles in the ISCs. Various morphology changes can be observed in Fig. 3a and b. The obvious contrast change in Fig. 3a suggests the melting of the separators around the nail. The diameters of the melted regions reached several millimeters, which are much larger than that of the nail tip (~0.31 mm). S5 and S6 were not penetrated. The black substances on S5 were materials from the laminates. The morphology change of each of the separators may mainly depend on the temperature it has experienced. The damages in S0 and S1 are milder probably because they are closer to the cool cell surface. As the temperature continues to rise during the local ISC, a specific separator can experience morphology evolution similar to those observed from S0 to S3. The small and irregular pinholes like those in S0 could form due to mechanical effects and mild melting. At higher temperatures, small pinholes collapse to larger ones (image of S1). Small cracks form initially nearby the melting frontier probably because of the thermal shrinkage of the melted center region. Small cracks also grow to bigger ones, as can be seen in S2. Further higher and wider temperature rise can finally give rise to the rupture and tearing of the melted region, evidenced by the images of S3 and S4. S1 was further examined by a scanning electron microscope (SEM) (Fig. 3b). Obvious solidification of the separator can be seen at the region close to the nail (region 2), suggesting very high temperature near the nail; wrinkles due to thermal shrinkage can be seen at a disconnected frontier (region 3); details of the cracks and rupture occurring at the melting frontier (region 5 and 6) were also seen more clearly. One notable finding is the obvious pore-closing behavior observed in the mildly melted region 4, as is in sharp contrast to the porous intact separator (region 1).

From Fig. 3c and d, it is obvious that the damages of the positive laminates are severe. The holes at P1 (diameter of 0.42 mm) and P2 (diameter of 0.76 mm) are much larger and irregular than those at N1 (0.36 mm) and N2 (0.2 mm), which may be evidence of the fusion and burn-out of the Al current collectors. The fusion of Al current collectors has also been predicted by previous studies [48,49]. This present research revealed that even in micro ISCs with cell voltage drops of several millivolts, Al fusion is prominent. Previously, we have deduced that Al fusion probably occurs at t1 and can alleviate the ISCs. Designing more sensitive current-interrupting collectors may thus be an effective strategy for preventing the micro ISC aggravation.

Moreover, as can be seen from Fig. 3c, large bowl-like pits are

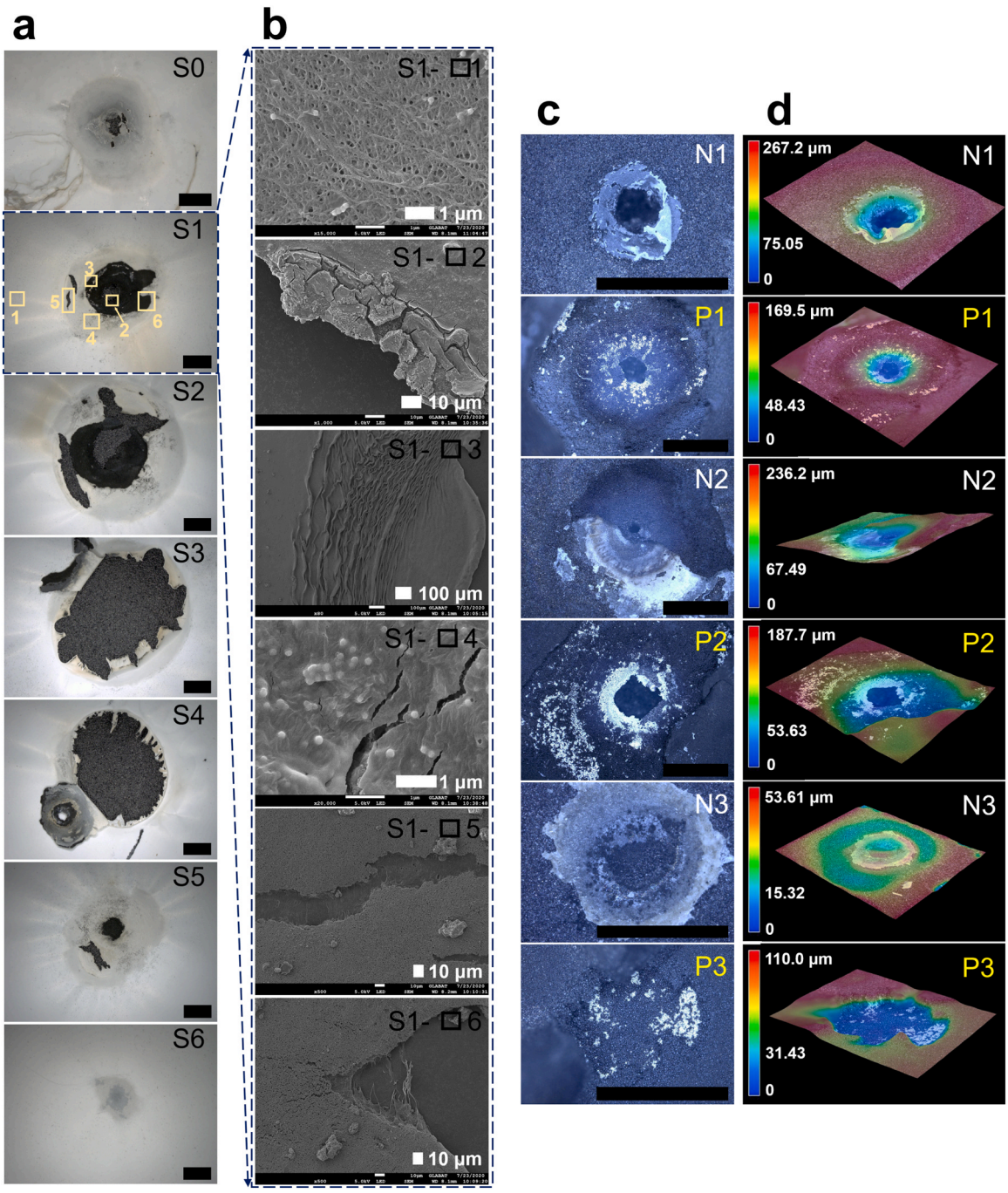

Fig. 3. (a) Optical images of the separators; (b) SEM images of the selected sections in sample S1 in (a); (c) optical and (d) reconstructed 3D images of the electrode laminates. The lengths of the black bars in the optical images are all 1 mm. The images are arranged in a way that mimics the arrangement of the separators and the electrode laminates in the cell. For instance, N1 is placed between S0 and S1. S0 is the outmost separator isolating the laminates from the Al plastic pouch.

obvious in P1 and P2 laminates, whereas N1 and N2 were almost intact except for regular nail holes. The more severe damage of the positive laminates may result from the higher joule heating caused by the much larger resistivity of the cathode coating layers (0.372 Ω m) than that of the anode coating layers (0.0645 Ω m). The destruction of the positive laminates may be caused by the heat-triggered gas-generating side reactions between the cathode and the electrolyte. And the wide destruction probably occurs around t2 in Fig. 2e, when the T-front reaches its maximum. The destruction of the positive laminates would increase the R_{PN} and impede the ISC current, which may contribute to the ISC alleviation and the voltage recovery from t2 to t3 in Fig. 2e.

3.2.3. *Micro ISC evolution mechanism*

The possible effects of the observed cell component behaviors on the ISC evolution are schematized in Fig. 4. Pinholes, cracks, rupture, and torn-off of the separators can enable direct local contacts of the electrodes and generate new ISC spots, which can play two roles. First, the directly shorted sub-sub cells precisely at the newly generated ISC spots can release their stored energy in short periods, as was evidenced by the abrupt voltage drop in the ARC test. This effect can cause instant but limited heat generation. Second, they can severe as current paths (like resistors) for other subcells and sub-sub cells to discharge and provide persistent joule heat until the whole cell depletes its energy. The pinhole and crack formation and enlargement may be responsible for the ISC

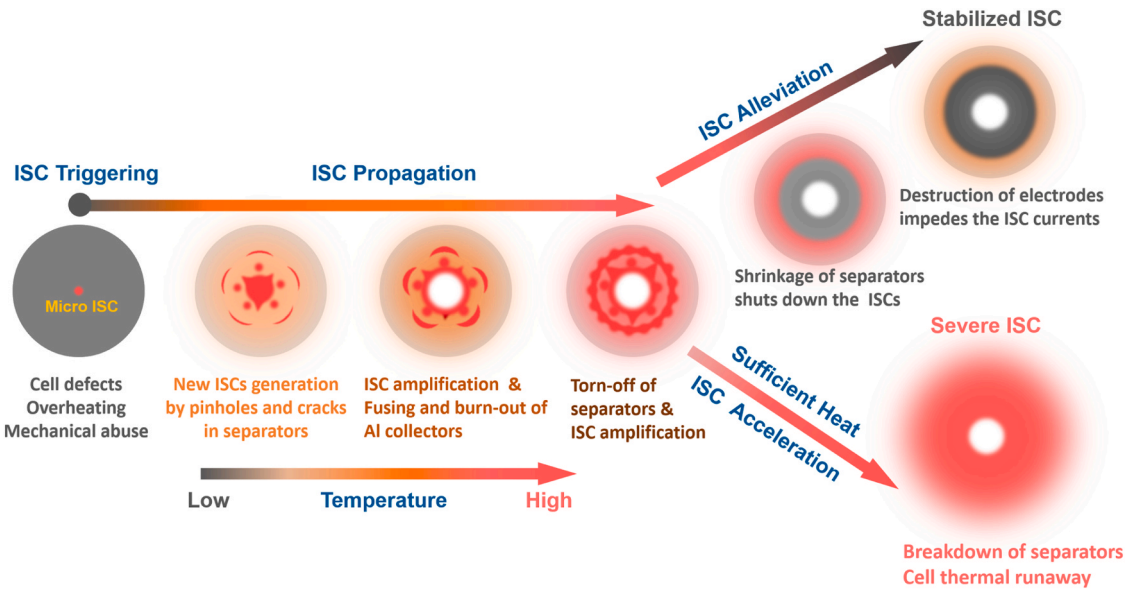

Fig. 4. Illustration of the mechanisms and crucial processes during the micro ISC triggering, propagation, alleviation, acceleration, and the cell thermal runaway.

propagation and the increasing ISC discharging current from t0 to t1 (Fig. 2e and f). The rupture and tearing of the melted center region may be the cause of the abrupt voltage drop and the ISC aggravation at t2 in the nail test (Fig. 2e). The voltage recovery from t2 to t3 may also have an association with the gradual shrinkage of the disconnected torn piece of the separators (S4 in Fig. 3a and N3 in Fig. 3c), which can partially close previously formed ISC spots. Combined with the alleviation role of the Al fusion and positive electrode destruction, as well as the decreased cell voltage, the heat generation might be not sufficient to support wider separator impairment spreading, which may lead to a stabilized micro ISC state.

In the ARC test, micro ISCs by the pinhole and crack formation in the separators are also likely to occur due to the high temperatures and the rough electrode laminate surfaces. However, the micro ISCs should occur numerously and distribute widely because of the uniform temperature environment, which may be accountable for the notable

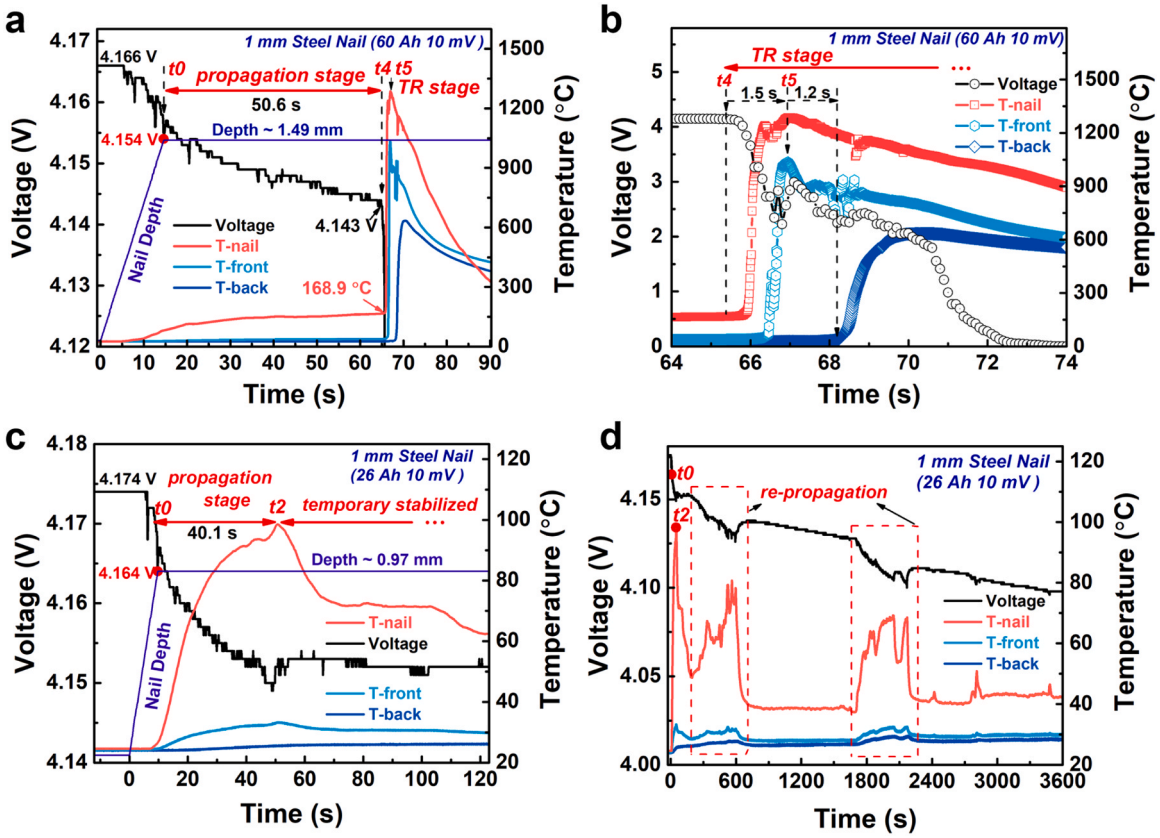

Fig. 5. Penetration depth, voltage, and temperature curves of the 60 Ah cell ((a) and (b)), and the 26 Ah cell ((c) and (d)) in the penetration tests with a 10 mV cut-off voltage drop. (b) is an enlarged section of (a); (d) is an enlarged section of (c).

voltage fluctuations at T_{MISC} (142 °C) in Fig. 1c. However, the voltage recovery in the ARC test cannot be due to the shrinkage of the torn pieces of the separators, which, if occurring widely, would cause the breakdown of the separators and result in large-area severe ISCs. We speculate that the voltage recovery can be attributed to the pore-closing behavior of the mildly melted separators, which can shut down the ionic flux and significantly increase the cell impedance to slow the cell discharging [50,51].

3.3. Micro ISC evolution to cell thermal runaway and effect of cell capacity

3.3.1. Micro ISC evolution to cell thermal runaway

We further set the cut-off voltage drop at 10 mV to trigger more aggressive micro ISCs. As can be seen in Fig. 5a, the nail stopped at 4.154 V, corresponding to an actual voltage drop of 12 mV and a penetration depth of 1.49 mm, much larger than that in the 5 mV cut-off test. From t0 to t4 (a period of 50.6 s), the voltage declines consistently and with some small fluctuations to 4.143 V; at the same time, the T-nail rose gradually to 168.9 °C. Voltage and temperature peaks observed in the 5 mV test are not obvious in the 10 mV test. We attribute this difference to the much more penetrated laminates and separators in the 10 mV test, which may not behave synchronously and can therefore smooth the voltage and temperature signals. The larger penetration depth provides a smaller ISC resistance and higher heat generation, which may give rise to the persistent ISC propagation and the continuously rising temperatures, finally exceeding the safe limit at t4. The accelerated voltage decline after t4 can be ascribed to the continuous rupture and breakdown of the separators. Side reactions between the active materials and the electrolyte may also be triggered. The T-nail and the T-front rapidly responded to the voltage drop and soared to their peaks ($\geq$ 1200 °C) in a very short time interval of about 1 s. Intense cell fire was observed. The small initial ISC voltage drop, short time interval, and extremely high temperature demonstrate the safety risk of the large-capacity HED cell in ISC events. SiO_x has been found advantageous for alleviating the ISC issue due to the nanosized SiO_2 matrix preventing anode side reaction [52] and the low electrically conductive SiO and Si after delithiation that could suppress the extension of ISC discharging [53]. Liu and Sakai et al. reported that a 1.16 Ah $LiFePO_4$/SiO laminated cell can pass the nail penetration test with negligible voltage and temperature changes [52]. However, probably due to the limited amount (ca. 12.5 wt%) of SiO_x in our anode material, the effect of SiO_x seems not sufficient to prevent the severe ISC and the cell TR. In another test, we used a high-speed video camera to capture the TR scene of the 60 Ah cell during the nail test, which is provided in the Supplementary Material (Video S1 and Fig. S4). Cell swelling, smoke, sparks, fire, and ejection of white-hot substances were clearly observed. We also performed a penetration test with a larger nail with a diameter of 3 mm and a tip cone angle of 45°. Because of the blunter nail tip and the mechanical effect, the voltage change was very abrupt and the nail failed to stop around the pre-set 5 mV cut-off. The cell went TR in a short period of less than 2.2 s (Fig. S5).

Supplementary material related to this article can be found online at doi:10.1016/j.nanoen.2021.105908.

3.3.2. Effect of cell capacity

Developing large-capacity cell is a widely used strategy to enhance the battery energy density by effectively deducing the weight contribution from the auxiliary cell components. Herein we investigate the effect of the cell capacity on the micro ISCs. The equivalent circuit analysis actually already provides some predictions. Since the ISC resistance in micro ISCs is generally much larger than the equivalent cell polarization resistance, the initial ISC situation and the ISC resistance dominates the magnitude of the ISC discharging current, the heat generation, and the severity of the ISC. However, cell polarization and voltage drop depend significantly on many cell parameters. Under identical currents, smaller-capacity cells generally develop larger polarization voltage drops. In other words, if identical voltage drops are detected by the BMS, the ISC currents in smaller-capacity cells will be smaller, the ISC resistance will be larger, and the penetration depth will be smaller. To verify these predictions, we performed a 10 mV cut-off penetration test on a 26 Ah cell with similar chemistry to the 60 Ah cell but fewer laminates.

As can be seen in Fig. 5c, the nail stopped at 4.164 V, corresponding to a voltage drop of 10 mV and a penetration depth of 0.97 mm, much smaller than that in the 60 Ah cell test (1.49 mm). This time the cell did not get fire and passed the test. Moreover, the curves in Fig. 5c are instead similar to those observed in the 5 mV test (Fig. 2e). The shorter time intervals and higher peaks imply more severe ISCs because of the deeper penetration depth than that in the 5 mV 60 Ah cell test (0.58 mm), which can also be verified by the additional couples of voltage and temperature peaks indicative of less stabilized ISC. The additional voltage and temperature peaks may arise from the variation of the contact resistances probably caused by the gas accumulation and venting. These observations and comparisons fully justify the equivalent circuit analysis and theoretical predictions. A smaller-capacity cell seems safer as the larger voltage drops from a similar micro ISC situation can be more easily recognized by the BMS. However, if the cells are connected in parallel in battery packs, spontaneous balancing between them would make the voltage drop signal from a single cell distorted and more undetectable. This analysis also emphasizes the importance of tracking the currents between cells connected in parallel to assist the identification and evaluation of micro ISCs.

4. Conclusions

In summary, this work investigates the micro ISC mechanism and safety risks in a 60 Ah HED pouch Li-ion cell. ARC and a high-precision penetration test were performed to trigger on-demand ISCs. The behaviors of the separators and electrode laminates during the early-stage micro ISCs were clearly captured and analyzed. While the pinholes, cracks, and ruptures of the separators can lead to new ISC spot formation and the ISC propagation, the pore-closing and shrinkage of the separators can shut down the ionic flux and the existing ISC spots, alleviating the ISCs. Even in micro ISCs, destruction of the positive electrodes and fusion of the Al current collectors are found to be prominent, which can impede the ISC current and also alleviate the ISCs. Moreover, these internal effects were correlated to the external voltage and temperature signals. It is found that voltage change signals even at millivolt level are noteworthy premonitory signals for warning of risky micro ISCs and can be used as leading indicators for predicting cell thermal runaway, while temperature signals are frequently lagged. It is also found that small-capacity cells are beneficial because of the larger ISC voltage drop signals that are more detectable by the BMS. These insights may shed some light on the micro ISC recognition, evaluation, warning, and prevention research.

CRediT authorship contribution statement

Xiaopeng Qi: Conceptualization, Investigation, Formal analysis, Writing - original draft. **Bingxue Liu**: Investigation, Formal analysis. **Jing Pang**: Supervision, Conceptualization. **Fengling Yun:** Resources, Investigation. **Rennian Wang**: Resources, Investigation, Project administration. **Yi Cui**: Resources, Methodology. **Changhong Wang**: Writing - review & editing, Formal analysis. **Kieran Doyle-Davis**: Writing - review & editing, Formal analysis. **Chaojian Xing**: Investigation. **Sheng Fang**: Resources. **Wei Quan**: Resources. **Bin Li**: Investigation. **Qiang Zhang**: Resources, Investigation. **Shuaijin Wu**: Resources, Investigation. **Shiyang Liu:** Resources, Investigation. **Jiantao Wang**: Supervision, Conceptualization. **Xueliang Sun**: Supervision, Conceptualization.

Declaration of Competing Interest

The authors declare that they have no known competing financial interests or personal relationships that could have appeared to influence the work reported in this paper.

Acknowledgements

This work was supported by the National Natural Science Foundation of China (Grant Nos 21903067 and 51604032); Beijing Natural Science Foundation (Grant No. L182023); and the National Key Research and Development Program of China (Grant No. 2016YFB0100509).

Appendix A. Supporting information

Supplementary data associated with this article can be found in the online version at doi:10.1016/j.nanoen.2021.105908.

References

[1] Z.P. Cano, D. Banham, S.Y. Ye, A. Hintennach, J. Lu, M. Fowler, Z.W. Chen, Batteries and fuel cells for emerging electric vehicle markets, Nat. Energy 3 (2018) 279–289.
[2] A. Kwade, W. Haselrieder, R. Leithoff, A. Modlinger, F. Dietrich, K. Droeder, Current status and challenges for automotive battery production technologies, Nat. Energy 3 (2018) 290–300.
[3] M.-T.F. Rodrigues, G. Babu, H. Gullapalli, K. Kalaga, F.N. Sayed, K. Kato, J. Joyner, P.M. Ajayan, A materials perspective on Li-ion batteries at extreme temperatures, Nat. Energy 2 (2017) 17108.
[4] X.N. Feng, D.S. Ren, X.M. He, M.G. Ouyang, Mitigating thermal runaway of lithium-ion batteries, Joule 4 (2020) 743–770.
[5] Z. Zhang, D. Fouchard, J.R. Rea, Differential scanning calorimetry material studies: implications for the safety of lithium-ion cells, J. Power Sources 70 (1998) 16–20.
[6] Y.-K. Sun, S.-T. Myung, B.-C. Park, J. Prakash, I. Belharouak, K. Amine, High-energy cathode material for long-life and safe lithium batteries, Nat. Mater. 8 (2009) 320–324.
[7] W.D. Li, E.M. Erickson, A. Manthiram, High-nickel layered oxide cathodes for lithium-based automotive batteries, Nat. Energy 5 (2020) 26–34.
[8] H. Wu, G. Chan, J.W. Choi, I. Ryu, Y. Yao, M.T. McDowell, S.W. Lee, A. Jackson, Y. Yang, L. Hu, Y. Cui, Stable cycling of double-walled silicon nanotube battery anodes through solid–electrolyte interphase control, Nat. Nanotechnol. 7 (2012) 310–315.
[9] J.R. Szczech, S. Jin, Nanostructured silicon for high capacity lithium battery anodes, Energy Environ. Sci. 4 (2011) 56–72.
[10] Q. Wang, P. Ping, X. Zhao, G. Chu, J. Sun, C. Chen, Thermal runaway caused fire and explosion of lithium ion battery, J. Power Sources 208 (2012) 210–224.
[11] H. Lee, M. Yanilmaz, O. Toprakci, K. Fu, X.W. Zhang, A review of recent developments in membrane separators for rechargeable lithium-ion batteries, Energy Environ. Sci. 7 (2014) 3857–3886.
[12] P. Arora, Z.M. Zhang, Battery separators, Chem. Rev. 104 (2004) 4419–4462.
[13] J. Kalhoff, G.G. Eshetu, D. Bresser, S. Passerini, Safer electrolytes for lithium-ion batteries: state of the art and perspectives, ChemSusChem 8 (2015) 2154–2175.
[14] Q.S. Wang, L.H. Jiang, Y. Yu, J.H. Sun, Progress of enhancing the safety of lithium ion battery from the electrolyte aspect, Nano Energy 55 (2019) 93–114.
[15] J. Sun, J.G. Li, T. Zhou, K. Yang, S.P. Wei, N. Tang, N.N. Dang, H. Li, X.P. Qiu, L. Q. Chen, Toxicity, a serious concern of thermal runaway from commercial Li-ion battery, Nano Energy 27 (2016) 313–319.
[16] V. Ruiz, A. Pfrang, A. Kriston, N. Omar, P. Van den Bossche, L. Boon-Brett, A review of international abuse testing standards and regulations for lithium ion batteries in electric and hybrid electric vehicles, Renew. Sustain. Energy Rev. 81 (2018) 1427–1452.
[17] R. Guo, L. Lu, M. Ouyang, X. Feng, Mechanism of the entire overdischarge process and overdischarge-induced internal short circuit in lithium-ion batteries, Sci. Rep. 6 (2016) 30248.
[18] B.H. Liu, Y.K. Jia, C.H. Yuan, L.B. Wang, X. Gao, S. Yin, J. Xu, Safety issues and mechanisms of lithium-ion battery cell upon mechanical abusive loading: a review, Energy Storage Mater. 24 (2020) 85–112.
[19] E. Sahraei, E. Bosco, B. Dixon, B. Lai, Microscale failure mechanisms leading to internal short circuit in Li-ion batteries under complex loading scenarios, J. Power Sources 319 (2016) 56–65.
[20] X.Q. Zhu, H. Wang, X. Wang, Y.F. Gao, S. Allu, E. Cakmak, Z.P. Wang, Internal short circuit and failure mechanisms of lithium-ion pouch cells under mechanical indentation abuse conditions: an experimental study, J. Power Sources 455 (2020), 227939.
[21] T. Yokoshima, D. Mukoyama, F. Maeda, T. Osaka, K. Takazawa, S. Egusa, Operando analysis of thermal runaway in lithium ion battery during nail-penetration test using an X-ray inspection system, J. Electrochem. Soc. 166 (2019) A1243–A1250.
[22] T. Yokoshima, D. Mukoyama, F. Maeda, T. Osaka, K. Takazawa, S. Egusa, S. Naoi, S. Ishikura, K. Yamamoto, Direct observation of internal state of thermal runaway in lithium ion battery during nail-penetration test, J. Power Sources 393 (2018) 67–74.
[23] X. Feng, M. Fang, X. He, M. Ouyang, L. Lu, H. Wang, M. Zhang, Thermal runaway features of large format prismatic lithium ion battery using extended volume accelerating rate calorimetry, J. Power Sources 255 (2014) 294–301.
[24] S. Santhanagopalan, P. Ramadass, J. Zhang, Analysis of internal short-circuit in a lithium ion cell, J. Power Sources 194 (2009) 550–557.
[25] T.G. Zavalis, M. Behm, G. Lindbergh, Investigation of short-circuit scenarios in a lithium-ion battery cell, J. Electrochem. Soc. 159 (2012) A848–A859.
[26] J. Zhu, T. Wierzbicki, W. Li, J. Power, A review of safety-focused mechanical modeling of commercial lithium-ion batteries, J. Power Sources 378 (2018) 153–168.
[27] F. Sun, R. Moroni, K. Dong, H. Markotter, D. Zhou, A. Hilger, L. Zielke, R. Zengerle, S. Thiele, J. Banhart, I. Manke, Study of the mechanisms of internal short circuit in a Li/Li cell by synchrotron X-ray phase contrast tomography, ACS Energy Lett. 2 (2017) 94–104.
[28] B. Zhang, Q.F. Wang, J.J. Zhang, G.L. Ding, G.J. Xu, Z.H. Liu, G.L. Cui, A superior thermostable and nonflammable composite membrane towards high power battery separator, Nano Energy 10 (2014) 277–287.
[29] Z. Chen, P.C. Hsu, J. Lopez, Y.Z. Li, J.W.F. To, N. Liu, C. Wang, S.C. Andrews, J. Liu, Y. Cui, Z.N. Bao, Fast and reversible thermoresponsive polymer switching materials for safer batteries, Nat. Energy 1 (2016) 8.
[30] L. Xia, S.-L. Li, X.-P. Ai, H.-X. Yang, Y.-L. Cao, Temperature-sensitive cathode materials for safer lithium-ion batteries, Energy Environ. Sci. 4 (2011) 2845–2848.
[31] X.N. Li, J.W. Liang, X.F. Yang, K.R. Adair, C.H. Wang, F.P. Zhao, X.L. Sun, Progress and perspectives on halide lithium conductors for all-solid-state lithium batteries, Energy Environ. Sci. 13 (2020) 1429–1461.
[32] J.N. Liang, J. Luo, Q. Sun, X.F. Yang, R.Y. Li, X.L. Sun, Recent progress on solid-state hybrid electrolytes for solid-state lithium batteries, Energy Storage Mater. 21 (2019) 308–334.
[33] X.F. Yang, J. Luo, X.L. Sun, Towards high-performance solid-state Li–S batteries: from fundamental understanding to engineering design, Chem. Soc. Rev. 49 (2020) 2140–2195.
[34] C.J. Orendorff, E.P. Roth, G. Nagasubramanian, Experimental triggers for internal short circuits in lithium-ion cells, J. Power Sources 196 (2011) 6554–6558.
[35] M.X. Zhang, J.Y. Du, L.S. Liu, A. Stefanopoulou, J. Siegel, L.G. Lu, X.M. He, X. Y. Xie, M.G. Ouyang, Internal short circuit trigger method for lithium-ion battery based on shape memory alloy, J. Electrochem. Soc. 164 (2017) A3038–A3044.
[36] D.P. Finegan, E. Darcy, M. Keyser, B. Tjaden, T.M.M. Heenan, R. Jervis, J.J. Bailey, R. Malik, N.T. Vo, O.V. Magdysyuk, R. Atwood, M. Drakopoulos, M. DiMichiel, A. Rack, G. Hinds, D.J.L. Brett, P.R. Shearing, Characterising thermal runaway within lithium-ion cells by inducing and monitoring internal short circuits, Energy Environ. Sci. 10 (2017) 1377–1388.
[37] S. Huang, X.N. Du, M. Richter, J. Ford, G.M. Cavalheiro, Z.J. Du, R.T. White, G. S. Zhang, Understanding Li-Ion cell internal short circuit and thermal runaway through small, slow and in situ sensing nail penetration, J. Electrochem. Soc. 167 (2020) 090526.
[38] H. Maleki, J.N. Howard, Internal short circuit in Li-ion cells, J. Power Sources 191 (2009) 568–574.
[39] K. Son, S.M. Hwang, S.G. Woo, J.K. Koo, M. Paik, E.H. Song, Y.J. Kim, Comparative study of thermal runaway and cell failure of lab-scale Li-ion batteries using accelerating rate calorimetry, J. Ind. Eng. Chem. 83 (2020) 247–251.
[40] I.A. Profatilova, T. Langer, J.P. Badillo, A. Schmitz, H. Orthner, H. Wiggers, S. Passerini, M. Winter, Thermally induced reactions between lithiated nano-silicon electrode and electrolyte for lithium-ion batteries, J. Electrochem. Soc. 159 (2012) A657–A663.
[41] I.A. Profatilova, C. Stock, A. Schmitz, S. Passerini, M. Winter, Enhanced thermal stability of a lithiated nano-silicon electrode by fluoroethylene carbonate and vinylene carbonate, J. Power Sources 222 (2013) 140–149.
[42] Q.S. Wang, J.H. Sun, X.L. Yao, C.H. Chen, Thermal behavior of lithiated graphite with electrolyte in lithium-ion batteries, J. Electrochem. Soc. 153 (2006) A329–A333.
[43] C. Shi, P. Zhang, L.X. Chen, P.T. Yang, J.B. Zhao, Effect of a thin ceramic-coating layer on thermal and electrochemical properties of polyethylene separator for lithium-ion batteries, J. Power Sources 270 (2014) 547–553.
[44] M. Mohamedi, H. Ishikawa, I. Uchida, In situ analysis of high temperature characteristics of prismatic polymer lithium - ion batteries, J. Appl. Electrochem. 34 (2004) 1103–1112.
[45] C.H. Yuan, L.B. Wang, S. Yin, J. Xu, Generalized separator failure criteria for internal short circuit of lithium-ion battery, J. Power Sources 467 (2020), 228360.
[46] X.W. Zhang, E. Sahraei, K. Wang, Li-ion battery separators, mechanical integrity and failure mechanisms leading to soft and hard internal shorts, Sci. Rep. 6 (2016) 32578.

[47] M.J. Chen, Q. Ye, C.M. Shi, Q. Cheng, B.Y. Qie, X.B. Liao, H.W. Zhai, Y.R. He, Y. Yang, New insights into nail penetration of Li-ion batteries: effects of heterogeneous contact resistance, Batter. Supercaps 2 (2019) 874–881.
[48] C.-S. Kim, J.-S. Yoo, K.-M. Jeong, K. Kim, C.-W. Yi, Investigation on internal short circuits of lithium polymer batteries with a ceramic-coated separator during nail penetration, J. Power Sources 289 (2015) 41–49.
[49] M.X. Zhang, L.S. Liu, A. Stefanopoulou, J. Siegel, L.G. Lu, X.M. He, M.G. Ouyang, Fusing phenomenon of lithium-ion battery internal short circuit, J. Electrochem. Soc. 164 (2017) A2738–A2745.
[50] G. Venugopal, J. Moore, J. Howard, S. Pendalwar, Characterization of microporous separators for lithium-ion batteries, J. Power Sources 77 (1999) 34–41.
[51] G. Venugopal, Characterization of thermal cut-off mechanisms in prismatic lithium-ion batteries, J. Power Sources 101 (2001) 231–237.
[52] Y.H. Liu, M. Okano, T. Mukai, K. Inoue, M. Yanagida, T. Sakai, Improvement of thermal stability and safety of lithium ion battery using SiO anode material, J. Power Sources 304 (2016) 9–14.
[53] A. Yamano, M. Morishita, M. Yanagida, T. Sakai, High-capacity Li-ion batteries using SiO-Si composite anode and Li-rich layered oxide cathode: cell design and its safety evaluation, J. Electrochem. Soc. 162 (2015) A1730–A1737.

Dr. Xiaopeng Qi is a senior engineer in China Automotive Battery Research Institute Co., Ltd. He got his B.S. in Applied Physics from Northwestern Polytechnical University (China) in 2008 and received his Ph.D. degree in Physics from Technical Institute of Physics and Chemistry, Chinese Academy of Sciences, in 2013. His research interests include safety and failure mechanisms of Li-ion batteries, and electrochemical synthesis of energy storage and conversion materials.

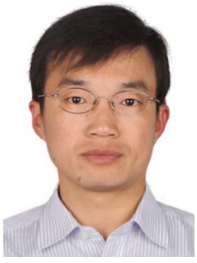

Dr. Bingxue Liu is a senior engineer in China Automotive Battery Research Institute Co., Ltd. He obtained his B.S. degree in Polymer Materials in 2004 and Ph.D. degree in Material Science in 2011 from Beijing University of Chemical Technology. His research interests focus on design and application of polymeric materials, additives and electrolyte towards safe Li-ion batteries.

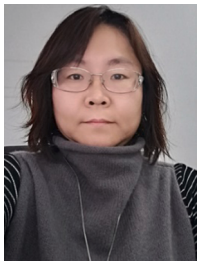

Prof. Jing Pang is a technical director in China Automotive Battery Research Institute Co., Ltd., and a professor in General Research Institute for Nonferrous Metals. She received her Ph.D. degree in Metallurgy of Non-ferrous Metals in 2004 from General Research Institute for Nonferrous Metals. Her current research interests focus on advanced electrode materials, and R&D of high-energy-density Li-ion batteries.

Dr. Fengling Yun is a senior engineer in China Automotive Battery Research Institute Co., Ltd. She received her Ph.D. in Non-ferrous Metallurgy from General Research Institute for Nonferrous Metals in 2016, after which she has been working on thermal analysis of Li-ion batteries and battery materials. Her research interests include characterization, quantification and failure analysis of thermal runaway of Li-ion batteries during full lifecycles.

Dr. Rennian Wang is a senior engineer and the manager for industrial technologies in China Automotive Battery Research Institute Co., Ltd. He obtained his Ph.D. in Physical Chemistry from the Institute of Chemistry, Chinese Academy of Sciences, in 2017. His research interests are focused on the generic technologies of high-performance Li-ion battery R&D such as safety and failure mechanisms.

Dr. Yi Cui is a senior engineer and the manager for battery safety and reliability testing center in China Automotive Battery Research Institute Co., Ltd. He obtained his B.S. in Chemistry in Nankai University in 2007, and received his Ph.D. in Physical Chemistry from The National Center for Nanoscience and Technology, Chinese Academy of Sciences, in 2014. His research interests are focused on the characterization and evaluation technologies for the safety of batteries and battery systems.

Dr. Changhong Wang is currently a research scientist in GLABAT Solid-State Inc. Canada. He obtained his M.S. degree in Materials Engineering in 2014 from University of Science and Technology of China (USTC) and received his Ph.D. degree in Mechanical and Materials Engineering from the University of Western Ontario (UWO), Canada. He also served as a research assistant in Singapore University of Technology and Design (SUTD) from 2014 to 2016. Currently, his research interests include solid-state sulfide electrolytes, all-solid-state batteries, and bio-inspired artificial synapses.

Kieran Doyle-Davis received his Honours B.Sc. in Physics from McMaster University in 2018, with research focus on process optimization for lithium ion battery fabrication, and thin polymer films. Kieran is currently an MESc candidate at the University of Western Ontario under the supervision of Prof. Xueliang Sun. His current research interests include the development of next generation surface modified 3-D current collectors for both solution and solid-state lithium ion batteries.

Chaojian Xing is an engineer in China Automotive Battery Research Institute Co., Ltd. He obtained his M.S. in Chemistry from China University of Mining and Technology in 2007. He also served as a research assistant in Institute of Processes Engineering, Chinese Academy of Sciences, from 2007 to 2013. His current research interests include the characterization and evaluation of the safety and reliability of Li-ion batteries.

Dr. Sheng Fang is a senior engineer in China Automotive Battery Research Institute Co., Ltd. He obtained his B.S. in Chemistry from Central China Normal University in 2010, and Ph.D. degree in Metallurgical Engineering in General Research Institute for Nonferrous Metals in 2015. His current research interests include molten salt electrolysis, high-capacity electrode materials, and safety of Li-ion batteries.

Shuaijin Wu is an engineer in China Automotive Battery Research Institute Co., Ltd. She received her B.S. from North China Electric Power University, and her M.S. in Materials Science and Engineering from General Research Institute of Nonferrous Metal in 2018. Her research interests focus on silicon anode electrode materials and electrode design for high-energy Li-ion batteries.

Dr. Wei Quan is a senior engineer in China Automotive Battery Research Institute Co., Ltd. He obtained his B.S. in Material Physics from Wuhan University of Technology in 2010, M.S. in Condensed Matter Physics from Beihang University in 2015, and Ph.D. degree in Material Science and Engineering from Tsinghua University in 2017. His research interests mainly focus on high-energy automotive Li-ion battery R&D and high-voltage electrolytes.

Shiyang Liu is now working as a research assistant in China Automotive Battery Research Institute Co., Ltd. He received his B.Eng. in 2016 from Xiamen University and gained his M.S. degree in 2018 from the University of Florida. His research interests focus on evaluation method of Li-ion batteries.

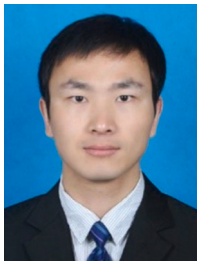

Bin Li is an engineer in China Automotive Battery Research Institute Co., Ltd. He obtained his M.S. in Mechanical Engineering from China University of mining and technology (Beijing) in 2014. His research interests focus on mechanical behavior of high-energy Li-ion batteries containing high-capacity electrode materials such as silicon anodes and high-nickel NCM cathodes.

Prof. Jiantao Wang is the general manager of Department of Innovation in China Automotive Battery Research Institute Co., Ltd, recipient of 2015 Beijing Nova program, professor in General Research Institute for Nonferrous Metals. He obtained his B.S. in Analytical Chemistry from University of Science and Technology Beijing in 2006, and received his Ph.D. in Organic Chemistry in Technical Institute of Physics and Chemistry, Chinese Academy of Sciences, in 2011. His research interests include advanced electrode materials, high-energy Li-ion batteries and solid-state batteries.

Qiang Zhang is an engineer in China Automotive Battery Research Institute Co., Ltd. He obtained his B.S. in Chemistry in 2013 and M.S. in Materials Physics and Chemistry in 2016 from Nankai University. His research interests focus on design and manufacture of high-energy-density Li-ion batteries.

Prof. Xueliang (Andy) Sun is a Canada Research Chair in Development of Nanomaterials for Clean Energy, Fellow of the Royal Society of Canada and Canadian Academy of Engineering and Full Professor at the University of Western Ontario, Canada. Dr. Sun received his Ph.D. in materials chemistry in 1999 from the University of Manchester, UK, which he followed up by working as a postdoctoral fellow at the University of British Columbia, Canada and as a Research Associate at L′ Institut National de la Recherche Scientifique (INRS), Canada. His research interests are focused on advanced materials for electrochemical energy storage and conversion.